2nd International Conference on Scientific and Academic Research
March 14-16, 2023 : Konya, Turkey
All Sciences Proceedings
http://as-proceeding.com/

The traditional control of Brushless Doubly-Fed Reluctance Machines

Oualah Oussama [1], Kerdoun Djallel [1] and Boumassata Abderraouf [2]

[1]LGEC Research Laboratory, Department of Electrical Engineering, Brothers Mentouri University Constantine 1, Constantine, Algeria
[2]National Polytechnic School Constantine, Algeria

oussama.oulha@umc.edu.dz Email of the corresponding author

Abstract **–**The conventional reluctance machine is poor in performance. Researchers have tried to improve it and have come out with a brushless doubly fed reluctance machine (BDFRM) which can run as a motor or generator. This machine is an attractive alternative in variable speed drives and wind power generation. The paper is concerned with flux and voltage vector-oriented control of a promising brushless doubly-fed reluctance machine (BDFRM) for generator and drive systems with limited adjustable speed ranges (e.g. wind turbines and/or pump drives).

Keywords –Vector Control (VC), Brushless Doubly Fed Reluctance Machine (BDFRM).

I. INTRODUCTION

An inverter-fed brushless doubly fed reluctance machine (BDFRM) is undoubtedly an attractive candidate for medium performance variable speed applications due to its low cost, high reliability and lower harmonic injection into the supply mains. The economic benefits and improved power quality of the BDFRM drive can be attributed to the machine's slip power recovery property implying the use of a smaller inverter (relative to the machine rating)[1] the brushless doubly-fed machines (BDFMs) have been considered for wind generators and pump-alike devices which have traditionally been served by a wound rotor induction machine with a controllable rotor resistance or dual supply (DFIM),the BDFM should retain the DFIM cost benefits of using a smaller inverter (e.g. around 25% of the machine rating, contributing further with higher reliability and maintenance-free operation by the absence of brush gear) [2]. The BDFRM shares all the advantages of doubly-fed machines over singly excited counterparts – the operational mode flexibility, the greater control freedom and the possibility of sub-synchronous and super-synchronous speed operation in both motoring and generating regimes.[3] The BDFIM/RM has two stator windings of different pole numbers and generally different applied frequencies (Fig. 1)—the primary (power) winding is grid connected and the secondary (control) winding is converter fed. Magnetic coupling between the windings, a prerequisite for torque to be produced from the machines, is provided via the rotor having half the total number of stator poles.5 In the BDFIM case, the rotor is of special cage construction composed of nested loops , whereas the BDFRM can use any of the Syncrel's rotor designs. In many respects, the BDFRM and the BDFIM are obviously similar, however, the BDFRM has the following important advantages[4].

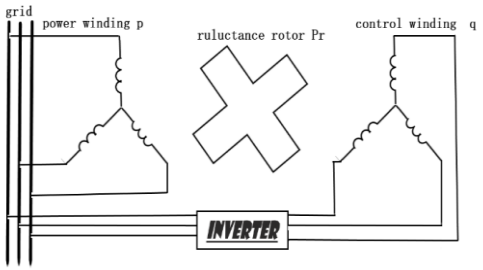

Fig. 1. A conceptual diagram of the inverter-fed BDFRM

The schematic representation of BDFRM is shown in Fig.1. It is seen that the winding wound for p number of poles which is connected to nearby grid and excited by normal power frequency supply called as power or primary winding. Other winding wound for q poles is excited either by a dc source or by a variable frequency, variable voltage source. The interaction of two magnetic fields produced by stator currents produces electromagnetic torque in the machine [5].

The paper gives a thorough review of the main control methods for the BDFRM. While the material to be presented is not new, it is comprehensive in nature and as such can certainly serve as a good reference for control related research for BDFRM , Vector control principles are also briefly discussed for entity of analysis, and to allow the interested reader to gain as global insight into the machine control properties as possible. A detailed consideration of a field-oriented control scheme, similar to the one presented in the paper, and aspects of its practical implementation for both motoring and generating modes of the BDFRM can be found in [1].

II. MATHMETICAL MODEL OF BDFRM

The basic mathematical equations of the BDFRM make are necessary in order to analysis and simulate the control algorithms of the BDFRM. This section will explain the mathematical model of the BDFRM. In basic form, the BDFRM stator model is similar to the induction machine, but it has two sets of three phase windings, and these have different pole numbers. The magnetic coupling between the two sets of windings is due to the rotor reluctance and the pole number selection is critical. The number of salient poles on the rotor should equal the average of the two stator windings. For instance, for a 2/6 stator pole machine it would have 4 pole and for a 4/8 stator pole machine it would have 6 poles. The machine should not have a stator pole pair different by one (i.e., 4/6 stator poles) because this will generator unbalanced magnet pull [6].

The space-vector voltage and flux equations for the machine in a stationary reference frame using standard notation and assuming motoring conventionareas follows[7].

$$\begin{cases} Vpd = R_P I_{pd} + \frac{d\Phi_{pd}}{dt} - \omega\phi_{pq} \\ Vpq = R_P I_{pq} + \frac{d\Phi_{pq}}{dt} + \omega\phi_{pd} \\ Vsd = R_s I_{sd} + \frac{d\Phi_{sd}}{dt} - (\omega_r - \omega)\phi_{sq} \\ Vsq = R_s I_{sq} + \frac{d\Phi_{sq}}{dt} + (\omega_r - \omega)\phi_{sd} \end{cases} \quad (1)$$

$$\begin{cases} \phi_{pd} = L_P I_{pd} + L_m I_{sd} \\ \phi_{pq} = L_P I_{pq} - L_m I_{sq} \\ \phi_{sd} = L_s I_{sd} + L_m I_{pd} \\ \phi_{sq} = L_s I_{sq} - L_m I_{pq} \end{cases} \quad (2)$$

The above flux equations can be manipulated to:

$$\begin{cases} \underline{\boldsymbol{\phi}_p} = \underbrace{\boldsymbol{L_P I_{pd}} + \boldsymbol{L_m I_{sd}}}_{\boldsymbol{\phi pd}} + \boldsymbol{j}.(\underbrace{\boldsymbol{L_P I_{pq}} - \boldsymbol{L_m I_{sq}}}_{\boldsymbol{\phi pq}}) \\ \underline{\boldsymbol{\phi_S}} = \boldsymbol{\sigma}\underbrace{\boldsymbol{L_s I_{sd}} + \boldsymbol{\phi_{ps_d}}}_{\boldsymbol{\phi sd}} + \boldsymbol{j}.\left(\boldsymbol{\sigma}\underbrace{\boldsymbol{L_s I_{sq}} + \boldsymbol{\phi_{ps_q}}}_{\boldsymbol{\phi sq}}\right) = \boldsymbol{\sigma L_s \underline{I_s}} + \frac{\boldsymbol{L_m}}{\boldsymbol{L_p}}\underline{\boldsymbol{\phi}}^*_{\boldsymbol{p}} \end{cases} \quad (3)$$

where $L_{p,s,m(ps)}$are the constant self and mutual three-phase inductances of the primary and secondary windings (their definitions can be found in [7]). In steady state, the machine develops useful torque.

The fundamental angular velocity and corresponding position relationships and torque for the machine torque production are:

$$\omega r = \omega_{rm} P_r = \omega_p + \omega_s \quad (4)$$

$$\omega_{rm} = \frac{\omega_p + \omega_s}{P_r} = \frac{(1-S).\omega_p}{p+q} = (1-s).\omega_{syn} \quad (5)$$

$$n_{rm} = 60\frac{f_p + f_s}{P_r} \quad (6)$$

$$\begin{cases} \omega_{rm} = \frac{d\theta_{rm}}{dt} \\ \omega_{p,s} = \frac{d\theta_{p,s}}{dt} \end{cases} \quad (7)$$

The mechanical equation of the system can be characterized by:

$$J.\frac{d\omega_{rm}}{dt} + f.\omega_{rm} = T_e - T_r \quad (8)$$

J is the inertia of the machine, f is the friction coefficient,

Tem is the electromagnetic torque and Tr is the load torque. The electromagnetic torque is expressed as:

$$T_e = \frac{3P_R L_m}{2L_P}(\phi_{pd} I_{sq} + \phi_{pq} I_{sd}) \quad (9)$$

Where the generalized slip is s= - ωs/ωp, and ωsyn =ωp/pr is the synchronous speed (for ωs=0) as with a 2pr-pole wound rotor synchronous turbo machine. If ωs>0 then the machine operates in super synchronous speed mode, else, i.e.for ωs<0 (e.g. the opposite phase sequence of the secondary winding to the primary one) when it is in sub-synchronous mode[8]

Using (5), one can derive the mechanical power equation showing individual contributions of each BDFRM winding:

$$P_m = T_e\omega_{rm} = \underbrace{\frac{T_e.\omega_p}{P_r}}_{P_p} + \underbrace{\frac{T_e.\omega_s}{P_r}}_{P_s} = P_p.\left(1+\frac{\omega_s}{\omega_p}\right) \quad (10)$$

The machine operating mode is determined by the power flow on the primary side i.e. from/to the grid for motoring (Te > 0) / generating (Te < 0), while the secondary can take or deliver real power subject to the winding phase sequence i.e. the ωs sign: the BDFRM would absorb (produce) positive secondary power at super (sub)-synchronous speeds as a motor, and at sub (super)-synchronous speeds as a generator.[9]

$$P_s = T_e\frac{\omega_s}{P_r} = P_P\frac{\omega_s}{\omega_p} = -sP_p \quad (11)$$

The power flow on the primary and secondary side of the machine assuming motoring convention as default are given in

visual form in Fig. 2 and summarised in Table 2.2 for both operating modes of the machine (motoring and generating) in super-synchronous and sub-synchronous speed regions.

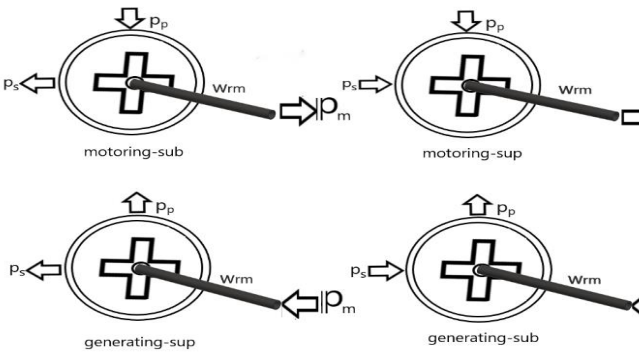

Fig. 2. Visualizing the BDFRM power flow for typical operating modes and speed regions.

Table.1. Power flows in case of positive and negative slip recovery modes

Speed Mode	**Motor Te>0**	**Generator Te<0**
Sub-synchronous($\omega s < 0$)	P_p>0 & P_s<0	P_p<0 & P_s>0
Super-synchronous($\omega s > 0$)	P_p>0 & Ps>0	P_p<0 & P_s<0

Preliminary simulation results for the machine direct on-line starting with the shorted secondary terminals are shown in Fig. 3 and Fig 4. Such an induction machine starting procedure is one possible way to prevent the inverter overloading (if partially-rated) during start-up . Using the construction design information of BDFRM together with parameter data allows testing the capability of the machine under various operating conditions[8].

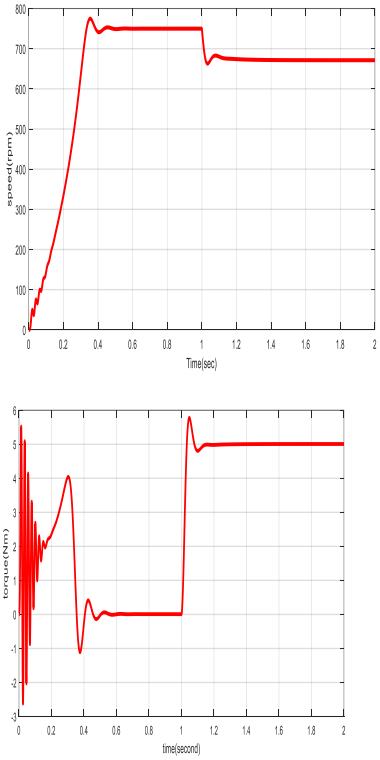

Fig. 3. Speed and electromagnetic torque starting transients.

III. Vector control

One of the most important advantages of the VC on a BDFRM is that the torque Te and primary winding reactive power Qp can be achieved in an inherently decoupled fashion. Here after, for most AC machines, special decoupling schemes are required

to eliminate crosscoupling effects between the d-q rotating frame control axes. This high-performance model-based control method allows much faster transient response, but an accurate knowledge of the BDFRM parameters, which can be obtained by off-line testing or estimated on-line, is necessary. For this reason, VC algorithms are more complicated and hence computationally more intensive (among other things, because of the reference frame conversion requirements) since DSP microcontroller implementation is imperative to achieve high control rate.[10]

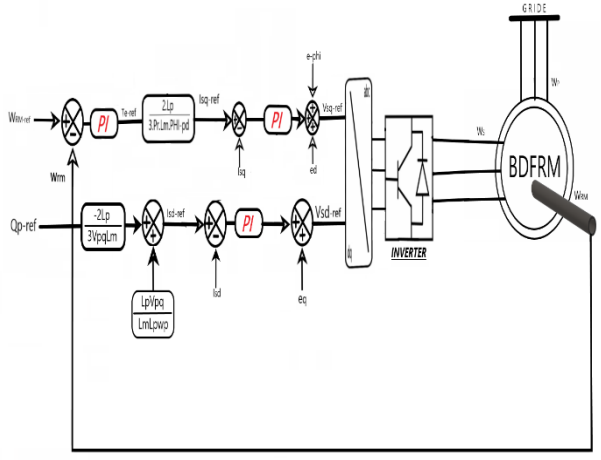

Fig. 4. Vector control diagram of the BDFRM.

In order to decouple the speed and the stator reactive power of the BDFRM, the primaire stator flux vector will be aligned with daxis φpd, (φpd = φp and φpq = 0), and the stator voltages will be expressed by :

$$\begin{cases} V_{pd} = 0 \\ V_{pq} = \omega_p . \phi_p \end{cases} \quad (12)$$

The expressions of the primaire stator currents are written as:

$$\begin{cases} I_{pd} = \frac{\phi_{pd} - L_m I_{sd}}{L_p} \\ I_{pq} = \frac{L_m I_{sq}}{L_p} \end{cases} \quad (13)$$

By replacing these currents in the secondary stator fluxes equations, we obtain:

$$\begin{cases} \phi_{sd} = L_s \sigma I_{sd} + \frac{L_m}{L_p} \phi_{pd} \\ \phi_{sq} = \sigma L_s I_{sq} \end{cases} \quad (14)$$

The secondary stator voltages can be written according to the secondary stator currents as:

$$\begin{cases} V_{sd} = R_s I_{sd} + L_s \sigma \frac{dI_{sd}}{dt} + eq \\ V_{sq} = R_s I_{sq} + L_s \sigma \frac{dI_{sq}}{dt} + ed + e\varphi \end{cases} \quad (15)$$

With

$$\begin{cases} eq = -\omega_s \sigma L_s I_{sq} \\ ed = \omega_s \sigma L_s I_{sd} \\ e\varphi = \omega_s \frac{L_m}{L_p} \phi_p \end{cases} \quad (16)$$

The electromagnetic torque can be written as:

$$T_e = \frac{3 P_r L_m}{2 L_p} \phi_{pd} I_{sq} \quad (17)$$

And the primary stator reactive power Qp of the BDFRM is expressed by:

$$Q_p = \frac{3}{2} \frac{{V_{pq}}^2}{\omega_p L_p} - \frac{3}{2} V_{pq} \frac{L_m}{L_p} I_{sd} \quad (18)$$

Figure 8 represents the simplified diagram of the speed and the stator reactive power control.

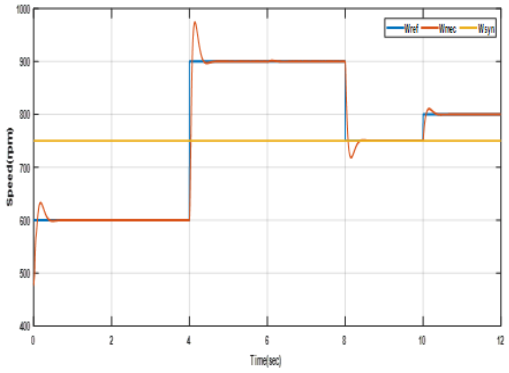

Fig. 5. Speed of the BDFRM

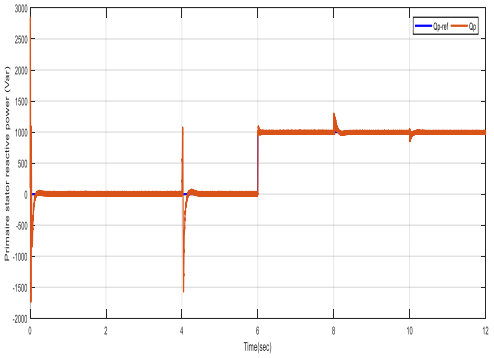

Fig. 6. the primary stator reactive power

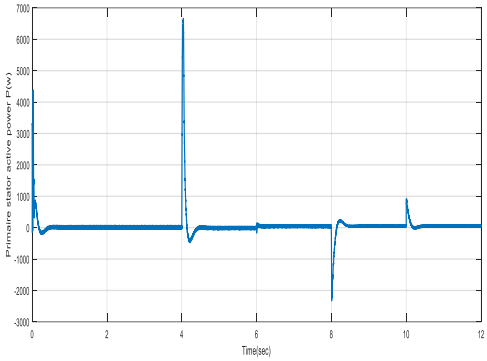

Fig. 7. the primary stator active power

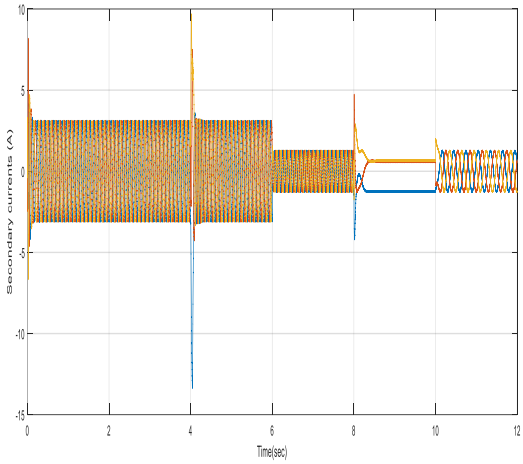

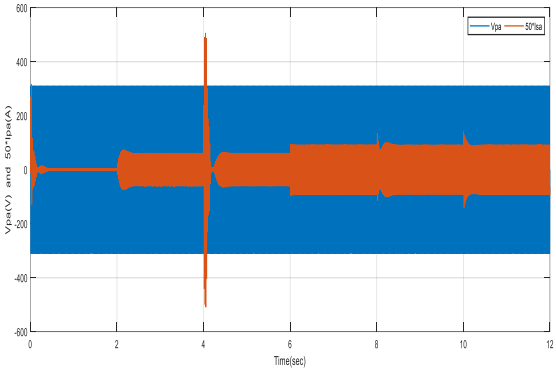

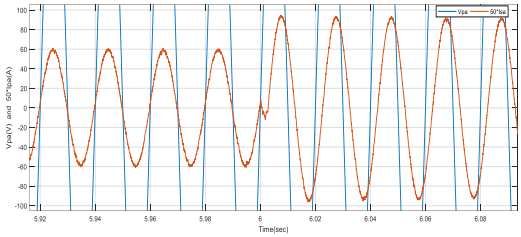

Fig. 8. primary stator phase voltage and currents and their zoom.

IV. RESULTS AND INTERPRETATIONS

Simulation of the proposed system was realized using MATLAB/Simulink. The BDFRM used in this work is 1.5 KW.It's connected directly to the line grid through its primary stator and controlled through it's second stator by a Inverter.

Rated parameters[11] : Vp = 380 V, fp = 50, Rp = 11.1 Ω, Rs = 13.5 Ω, Lp = 0.41 H, Ls = 0.57 H, Lm = 0.32 H, J = 0.1 Kg.m , and Pr = 4.

Figure 4 shows the excellent speed tracking for synchronous (750 rev/min), super-synchronous (900 rev/min) and sub synchronous (600 rev/min) operation of the BDFRM in the secondary frequency range of fs = ±10 Hz.

Figure 5 shows the primary stator reactive power of the BDFRM and its reference which varies from zero to 1000 Var at t = 6s.

The primary stator phase voltage and current and their zoom at a constant frequency of 50 Hz is given in Fig.7. The simple waveforms of the secondary stator currents and their zoom are shown in Fig. 13. Figure 14 illustrates the zoom of the secondary stator phase voltage and current and the secondary stator active power is given in Fig.8.

In Figs. 4 and 5, the BDFRM speed and primary stator reactive power follow their references correctly and validate the independent control using stator-flux oriented control technique. Moreover, the BDFRM in Fig.4 operates in three modes; the sub-synchronous mode ($\omega < \omega p$) is the first one ($0 < t < 4$ and $6 < 9$) and the second one is the super-synchronous mode ($\omega > \omega p$) ($4 < t < 8$ and $10 < 12$) and synchronous mode($\omega = \omega p$) ($8 < t < 10$) .

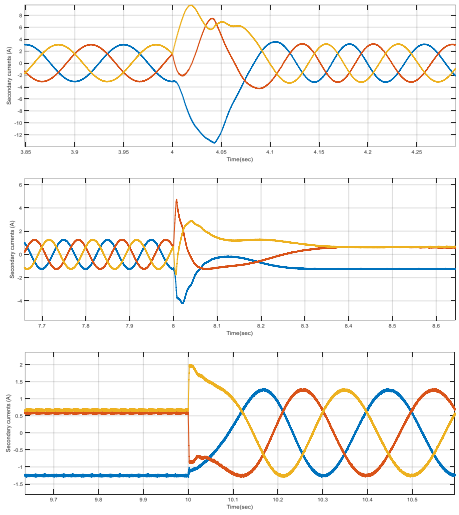

Fig. 9. Secondary currents and its zoom in the first and second and third transition respectively(a,b,c)

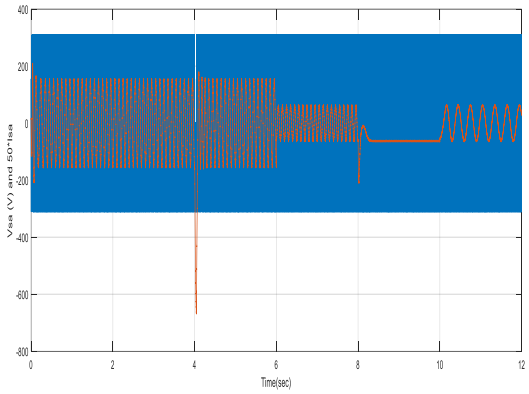

Fig. 9. secondary stator phase voltage and currents

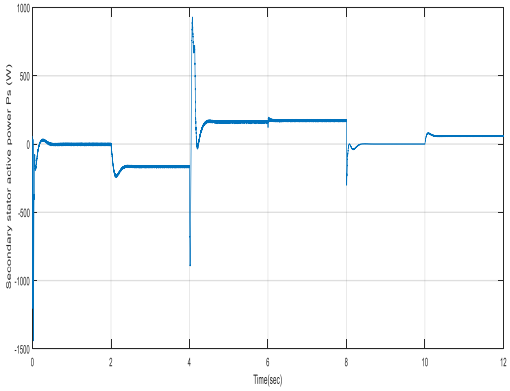

Fig. 10. The Secondary stator active power Ps (W)

It is clear in Fig. 7 that the phase between the primary stator phase voltage and current varies according to the variation of the stator reactive power (at t = 6s, Qp = 1000 Var).

In Fig.8, the frequency of the Secondary currents is low and varies according to the variation of the BDFRM speed.Fig.8(a) shows the first transition from sub-synchronous mode to super-synchronous mode and the second transition is in Fig.8(b) from super-synchronous mode to synchronous mode and the third transition is in Fig.8(c) from synchronous mode to super-synchronous mode.

The Secondary stator phase current and voltage shown in Fig. 9 validate the control of the inverter.

Figure 10 validates the operation of the three modes. In this figure the Secondary stator active power in the first mode ($0 < t < 4$) is negative because the Secondary stator provides power to the grid and in the second mode ($4 < t < 8$ and $10 < t < 12$) the Secondary stator active power is positive because the Secondary stator absorbs power from the grid and in the the third mode($8 < t < 10$) the Secondary stator active power is null.

V. CONCLUSTION

This paper presents at dynamic simulation model of BDFRM and the separate control of the speed and the stator reactive power of the brushless doubly fed reluctance machine through the inverter using MATLAB/Simulink®. The primary stator of the BDFRM is connected directly to the line grid while the Secondary stator is connected and controlled through three phase inverter. Simulation results show good decoupling and performance between speed and stator reactive power using stator-flux oriented control and cosine-wave crossing control techniques. They also demonstrate the ability to operate in the sub synchronous and super-synchronous modes. Moreover, the robustness quality of the proposed system appears clearly in the speed and the stator reactive power reference variations. So, this proposed system has proved the efficiency, demonstrated the performance and reduced the cost.

REFERENCES

[1] M. Jovanovic,2005,juin.Control of Brushless Doubly-Fed Reluctance Motors . in Proceedings of the IEEE International Symposium on Industrial Electronics, (pp. 1667-1672).

[2] S. Ademi et M. G. Jovanović,2015,janv. Vector Control Methods for Brushless Doubly Fed Reluctance Machines . IEEE Transactions on Industrial Electronics(pp. 96-104).

[3] M. G. Jovanovic et R. E. Betz,2000.Power factor control using brushless doubly fed reluctance machines.in Conference Record of the 2000 IEEE Industry Applications Conference. Thirty-Fifth IAS Annual Meeting and World Conference on Industrial Applications of Electrical Energy (Cat. No.00CH37129), Rome, Italy(p. 523-530).

[4] M. G. Jovanovic, R. E. Betz, et Jian Yu,2002,nov. The use of doubly fed reluctance machines for large pumps and wind turbines. IEEE Transactions on Industry Applications (pp. 1508-1516).

[5] S. Kunte, M. Bhawalkar, N. Gopalakrishnan, et Y. P. Nerkar,2016,sept. Brushless doubly fed reluctance machine and its control . in 2016 International Conference on Automatic Control and Dynamic Optimization Techniques (ICACDOT) (pp. 667-672).

[6] W. K. Song et D. G. Dorrell,2015,déc .Modeling and Simulation Study for Dynamic Model of Brushless Doubly Fed Reluctance Machine Using Matlab Simulink. in 2015 3rd International Conference on Artificial Intelligence, Modelling and Simulation (AIMS) (pp 382-386)

[7] R.E. Betz et Miluton Jovanovic, 1998,march .Introduction to Brushless Doubly Fed Reluctance Machines – The Basic Equations .

[8] BOUMASSATA, A., KERDOUN, D., et OUALAH, O. Maximum power control of a wind generator with an energy storage system to fix the delivered power. *Electrical Engineering & Electromechanics,(2)*, 2022, p. 41-46.S. Ademi, M. G. Jovanović, et M. Hasan,2015,juin.Control of Brushless Doubly-Fed Reluctance Generators for Wind Energy Conversion Systems. IEEE Transactions on Energy Conversion(pp 596-604).

[9] S. Ademi et M. Jovanovic,2012,juin.Vector control strategies for brushless doubly-fed reluctance wind generators.in 2012 2nd International Symposium On Environment Friendly Energies And Applications(pp 44-49).

[10] OUALAH, O., KERDOUN, Djallel, et BOUMASSATA, Abderraouf. Comparative study between sliding mode control and the vector control of a brushless doubly fed reluctance generator based on wind energy conversion systems. *Electrical Engineering & Electromechanics,(1)*, 2022, p. 51-58.